Extended Hückel Molecular-orbital Calculations on Dodecahedral Metalloboranes which do not conform to the Polyhedral Skeletal Electron-pair Theory

By **David N. Cox** and **D. Michael P. Mingos,*** Inorganic Chemistry Laboratory, University of Oxford, South Parks Road, Oxford OX1 3QR
Roald Hoffmann, Department of Chemistry, Cornell University, Ithaca, New York 14853, U.S.A.

Extended Hückel molecular-orbital calculations on the model complexes $[B_4H_4(CoL_3)_4]^{4+}$ and $B_4H_4(CoL_3)_4$, where L = a two-electron σ-donor ligand, have established the electronic factors responsible for the breakdown of the polyhedral skeletal electron-pair theory when applied to $B_4H_4[Co(\eta\text{-}C_5H_5)]_4$ and $B_4H_4[Ni(\eta\text{-}C_5H_5)]_4$. In addition the observation that $B_4H_4[Co(\eta\text{-}C_5H_5)]_4$ and $B_4H_4[Ni(\eta\text{-}C_5H_5)]_4$ adopt alternative D_{2d} structures based on the dodecahedron has been rationalised in terms of the different electronic requirements for stabilising the flattened metal tetrahedral structure in $B_4H_4[Co(\eta\text{-}C_5H_5)]_4$ and the elongated metal tetrahedral structure in $B_4H_4[Ni(\eta\text{-}C_5H_5)]_4$.

In recent years the synthesis of a wide range of polyhedral carbametalloboranes particularly by Hawthorne,[1] Grimes,[2] and Stone,[3] and their co-workers has added a new and exciting dimension to organometallic chemistry. The development of new synthetic pathways to these complex three-dimensional molecules has been accompanied by the development of simple electron-counting rules which have been used to predict and rationalise the polyhedral geometries adopted by a large majority of the known compounds.[4] The theoretical basis and applications of these rules have been widely reviewed and the reader is referred to refs. 5—10 for a fuller discussion of the *isolobal principle*, and the interactions between B–H, C–H, and $M(\eta\text{-}C_5H_5)$ fragments in spherical and capped polyhedral molecules.

In previous papers we have discussed [11–15] how extended-Hückel molecular-orbital calculations may be used to rationalise distortions within this class of polyhedral molecule and in particular the *slip* distortion in metal complexes of carbaboranes and thiaboranes. In addition, the limitations of the simple electron-counting rules in triple-decker sandwich compounds derived from hydrocarbons have been noted.[16] In this paper a more dramatic illustration of the breakdown of the electron-counting rules will be analysed in some detail. *X*-Ray crystallographic studies of the $B_8H_8^{2-}$ ion [17] have demonstrated that in the solid state this ion has the D_{2d} Δ-dodecahedral structure illustrated in Figure 1(*a*). In solution this ion undergoes very facile polyhedral rearrangement processes and it was proposed that in donor solvents the preferred ground-state structure for the $B_8H_8^{2-}$ ion is either a bicapped trigonal prism or a square antiprism.[18,19] However, recent calculations have indicated that the rearrangement may proceed through a C_{2v} structure formed by breaking only one of the B–B bonds.[20] On the basis of the polyhedral skeletal electron-pair theory [4–10] it would be predicted that $[B_4H_4\{Co(\eta\text{-}C_5H_5)\}_4]^{2-}$ and $[B_4H_4\{Ni(\eta\text{-}C_5H_5)\}_4]^{2+}$ should have similar Δ-dodecahedral polyhedral geometries since B–H, $Co(\eta\text{-}C_5H_5)$, and $Ni(\eta\text{-}C_5H_5)^+$ are all isolobal and pseudo-isoelectronic. Recently, Grimes and co-workers [21,22] have reported the syntheses of the neutral derivatives $B_4H_4[M(\eta\text{-}C_5H_5)]_4$, where M = Co or Ni, from reactions (1) and (2).

$$B_5H_8^- + Na[C_5H_5] + CoCl_2 \longrightarrow \underset{(I)}{B_4H_4[Co(\eta\text{-}C_5H_5)]_4} + \text{other products} \quad (1)$$

$$B_5H_8^- + Na/Hg + [Ni(C_5H_5)_2] \longrightarrow \underset{(II)}{B_4H_4[Ni(\eta\text{-}C_5H_5)]_4} + \text{other products} \quad (2)$$

The *X*-ray crystallographic analyses of (I) and (II) as illustrated in Figure 1(*b*) and (*c*) show that although both

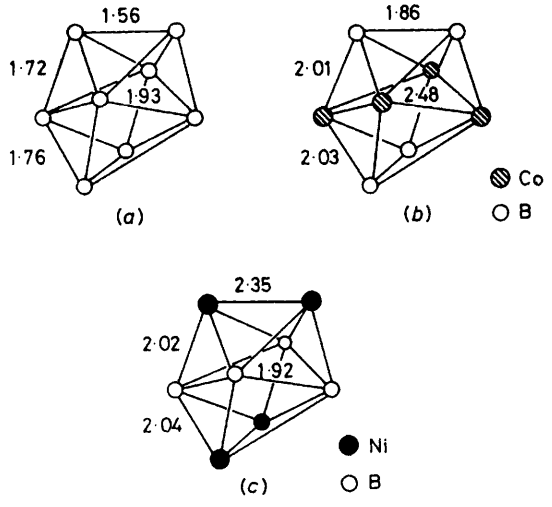

FIGURE 1 Molecular geometry of (*a*) $B_8H_8^{2-}$,[17] (*b*) $B_4H_4[Co(\eta\text{-}C_5H_5)]_4$,[20] and (*c*) $B_4H_4[Ni(\eta\text{-}C_5H_5)]_4$.[21] Bond lengths in Å

compounds contain the same basic dodecahedral architecture and belong to the D_{2d} point group they differ in an important and intriguing fashion. In the cobalt complex [Figure 1(*b*)] the metal atoms occupy the high-connectivity sites of the dodecahedron, whereas in the nickel complex [Figure 1(*c*)] the metal atoms occupy the low-connectivity sites. Interestingly, neither structure

shows large departures from the idealised *closo*-dodecahedral structure. Such distortions would have been anticipated for molecules which have two electrons too few and two electrons in excess of that predicted by the polyhedral skeletal electron-pair theory. The only minor irregularity noted was that, in the nickel complex, the nickel–nickel distances were shorter than those previously reported for comparable carbametalloboranes.

In this paper we report extended-Hückel molecular-orbital calculations (details of which are described in the Appendix) which account for the anomalous electron counts in these molecules and the preferred site occupations of the metal atoms.

RESULTS AND DISCUSSION

In analysing the bonding in $B_8H_8^{2-}$ and the related substituted metalloborane derivatives $B_4H_4[M(\eta\text{-}C_5H_5)]_4$, a strategy which fully utilises the D_{2d} symmetry of all three molecules and clearly distinguishes between high- and low-connectivity sites was adopted. It originates from the realisation that the dodecahedron may be viewed as the fusion of two independent but D_{2d} distorted tetrahedra (incidentally this observation is well recognised by mathematicians who describe the Δ-dodecahedron as a *Siamese Dodecahedron*). The combination of an elongated tetrahedron (E) and a flattened tetrahedron (F) which generates a Δ-dodecahedron is illustrated in Figure 2. The important skeletal molecular

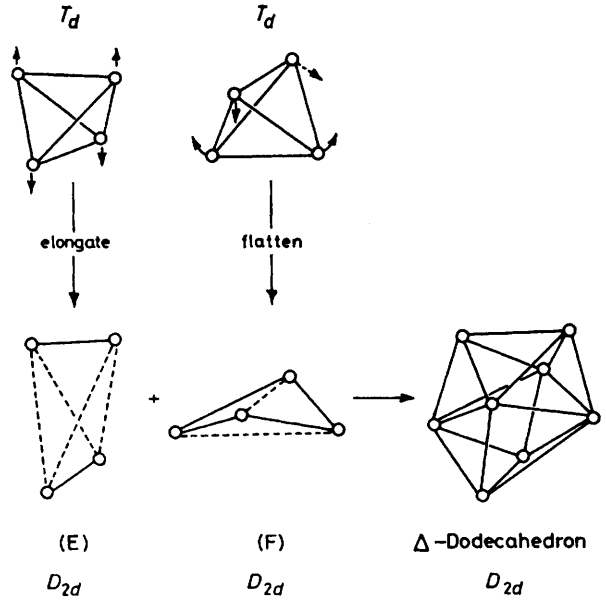

FIGURE 2 Conceptual formation of a Siamese Δ-dodecahedron from two distorted tetrahedra of D_{2d} symmetry. One is elongated (E) and one flattened (F)

orbitals of $B_8H_8^{2-}$ and $B_4H_4[M(\eta\text{-}C_5H_5)]_4$ are derived by taking the appropriate linear combinations of molecular orbitals of the isolated elongated and flattened B_4H_4 and $M_4(\eta\text{-}C_5H_5)_4$ tetrahedral entities. The extent of distortion from the idealised tetrahedral geometries may be appreciated from the fact that in $B_8H_8^{2-}$ the elongated tetrahedron has dimensions of 1.56 (2) and 2.81 (4) Å and the flattened tetrahedron has dimensions of 1.93 (4) and 2.53 (2) Å.*

An Evaluation of D_{2d} Distortions in B_4H_4 Tetrahedra.—Before considering the interactions between the B_4H_4 tetrahedra in $B_8H_8^{2-}$ it is important to evaluate the effects of the D_{2d} distortions on the skeletal molecular orbitals of an idealised B_4H_4 tetrahedron. Figure 3 †

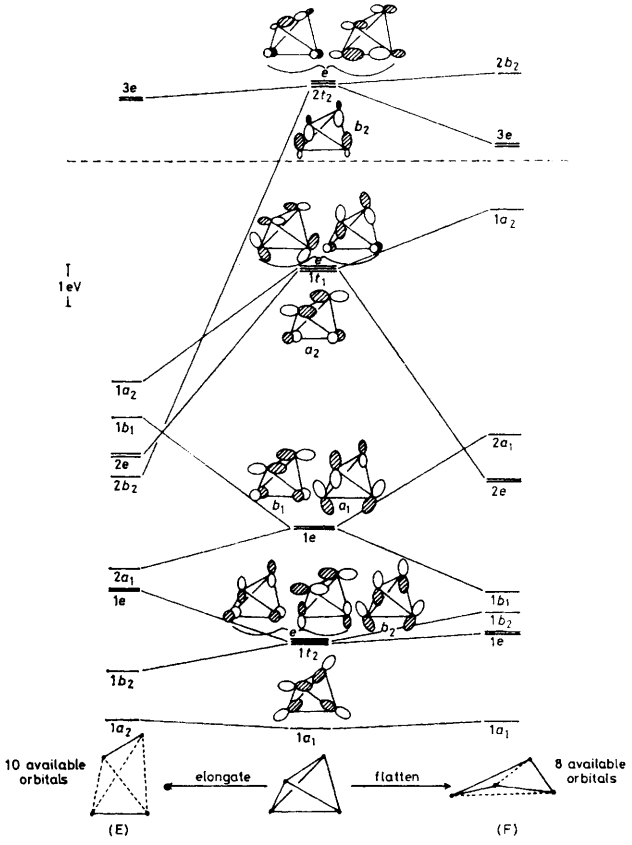

FIGURE 3 Effect of elongation and flattening on the skeletal molecular orbitals of a B_4H_4 tetrahedron

illustrates the bonding and antibonding skeletal molecular orbitals of tetrahedral B_4H_4. Similar schemes have been described for analogous molecules elsewhere [23,24] and therefore only those features relevant to the current discussion will be emphasised here. The skeletal bonding molecular orbitals of B_4H_4 transform as a_1, t_2, and e and the antibonding molecular orbitals as t_1 and t_2. The former bear a precise topological relationship to the six edges of the tetrahedron.[24] Figure 3 also illustrates the effects of introducing either a D_{2d} elongation or flattening distortion on the energies of these molecular orbitals. On lowering the symmetry from T_d to D_{2d} the degener-

* The figures in parentheses refer to the number of edges with these bond lengths.

† Although the arguments given in this paper rely heavily on symmetry considerations the Figures are derived from extended-Hückel calculations which are described in the Appendix.

acies of the molecular orbitals of B_4H_4 are lifted as shown below. It is apparent from Figure 3 that the

$$T_d \rightarrow D_{2d}$$
$$t_1 \rightarrow e, a_2$$
$$e \rightarrow a_1, b_1$$
$$t_2 \rightarrow e, b_2$$
$$a_1 \rightarrow a_1$$

molecular orbitals which experience the largest energy changes on distortion are the components derived from $1t_1$, $1e$, and $2t_2$. For the bonding $1t_2$ and $1e$ molecular orbitals the sense in which the degeneracy is removed is opposite for the elongated and flattened tetrahedra and the slopes of the energy levels in the Figure can be largely appreciated from a consideration of the relative phases of the contributing atomic orbitals across the edges of the tetrahedron. For example, when a D_{2d} flattening distortion is imposed on the $1e$ bonding set in B_4H_4 the b_1 molecular-orbital component is stabilised since the antibonding interactions across the two edges which have been lengthened are reduced and the bonding interactions across the remaining edges improved. These effects are represented schematically below. On the other hand the a_1 com-

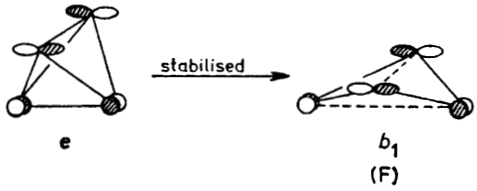

ponent of $1e$ is destabilised since the bonding interaction across the edges which have been lengthened is reduced and a stronger antibonding interaction is introduced across the remaining edges as shown below. Clearly for

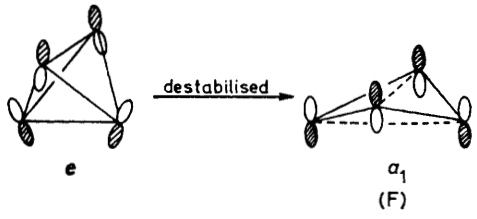

the elongated tetrahedron the effects will operate in the opposite fashion and the a_1 component is stabilised and the b_1 component destabilised. The $1t_2$ molecular orbitals show similar complementary effects (see Figure 3).

For the antibonding $1t_1$ and $2t_2$ molecular orbitals the effects of the distortion are much more dramatic since the diminution of atomic overlap integrals across specific edges will result in a larger first-order stabilisation for antibonding molecular orbitals. For the $1t_1$ set, a_2 and e components are generated by the removal of the degeneracy. In the flattened tetrahedron the e component is stabilised significantly by a decrease in the antibonding interactions illustrated below. In the

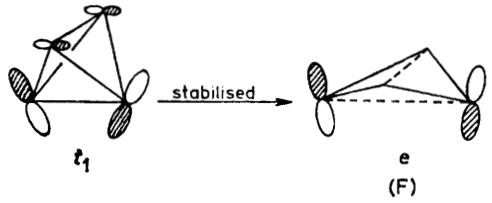

elongated tetrahedron a similar stabilisation results from a decrease of antibonding character across the four stretched edges as shown below.

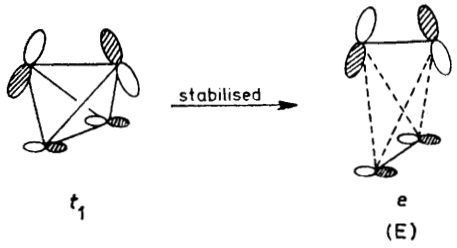

For the a_2 component there is a destabilisation in the case of the flattened tetrahedron and a stabilisation in the cases of the elongated tetrahedron. This difference can readily be appreciated in terms of the changes in the interatomic $2p$–$2p$ overlaps in the following schematic

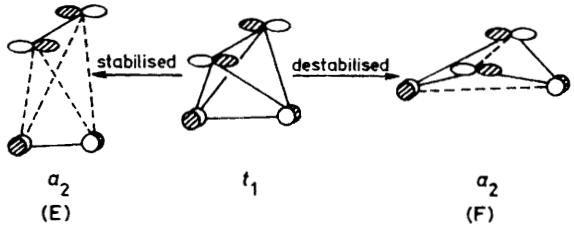

representation. In the flattened tetrahedron the decreased antibonding interaction along the edges which have been lengthened is outweighed by the increased antibonding interactions across the remaining edges. Consequently, the net effect is destabilising.

For the antibonding $2t_2$ set of B_4H_4, the energies of the molecular orbitals are so high-lying that in general their effects can be disregarded when relatively small distortions are under consideration. There is one exception, however. The b_2 component of the $2t_2$ set in the elongated tetrahedron experiences a remarkably large stabilisation and in the final distorted geometry has an energy comparable to that of the e component of the $1t_1$ molecular orbital. The $2t_2$ molecular orbital in B_4H_4 has an almost equal proportion of boron s and p character and the large stabilisation of the b_2 component in the elongated tetrahedron can be attributed to a substantial decrease in the out-of-phase overlap of the s orbitals. The b_2 component in the flattened tetrahedron experiences a loss of in-phase overlap. The important changes in the

interatomic 2*s*–2*s* overlaps arising from these distortions are represented schematically below.

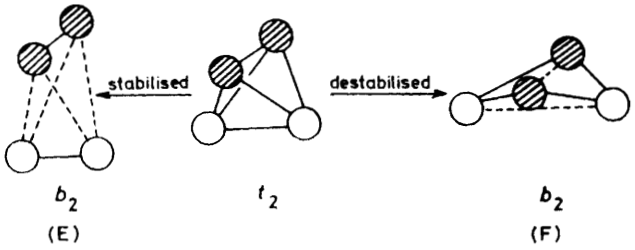

Before discussing in detail the way in which the frontier molecular orbitals of the elongated and flattened tetrahedra interact to form the dodecahedral $B_8H_8^{2-}$ polyhedron, it is perhaps worth digressing briefly to consider the electronic requirements necessary for stabilising these distorted polyhedral entities. The undistorted tetrahedral geometry is commonly associated with either four or six skeletal electron pairs as exemplified by B_4Cl_4 and P_4 respectively. In the former the electronic configuration is . . . $(1a_1)^2(1t_2)^6$ and in the latter . . . $(1a_1)^2(1t_2)^6(1e)^4$ (see Figure 3). From this Figure it is also apparent that neither of these electronic configurations provides a suitable basis for an energetically favourable distortion away from the idealised tetrahedron. Such distortions require the electron population of the higher-lying and antibonding $1t_1$ set of molecular orbitals and therefore will only be apparent for polyhedral molecules with more than six electron pairs. From Figure 3 the following distinct situations may be delineated.

(*a*) For a molecule with seven electron pairs, *e.g.* $C_4H_4^{2-}$ or Se_4^{2+}, a large flattening distortion which utilises the full stabilisation of the *e* component of t_1 and minimises the increased antibonding character of the a_1 component of the *e* molecular orbital is predicted. Indeed the observed planar geometry is calculated to be most stable since the maximum cyclic delocalisation is obtained for such a six-electron Hückel π system when the atoms are coplanar.

(*b*) For tetranuclear polyhedra with eight skeletal electron pairs the flattening distortion does not proceed to planarity since the additional electron pair compared with (*a*) above populates the a_1 component of *e* which is destabilised along the distortion co-ordinate. The equilibrium geometries for such compounds would therefore be expected to lie intermediate between tetrahedral and planar. Indeed this is found to be the case in molecules such as P_4Ph_4 which possess eight skeletal electron pairs.

(*c*) For the elongated tetrahedron the close proximity of the energy levels of b_2, *e*, b_1, and a_2 symmetry suggest that these levels will probably be occupied simultaneously, a situation which corresponds to the presence of 10 skeletal electron pairs. The final geometric consequence of such an elongation is complete dissociation of the tetrahedron into two diatomic molecules and indeed a hypothetical Cl_4 molecule would possess this number of skeletal electron pairs.

These conclusions are in themselves trivial and their general consequences have been discussed previously,[4b] but they serve to reinforce an important argument in understanding the bonding in the $B_4H_4[M(\eta\text{-}C_5H_5)]_4$ polyhedra, which also have eight and 10 skeletal electron pairs when M = Co and Ni respectively.

Molecular-orbital Analysis of $B_8H_8^{2-}$.—It has been known for some time, initially as a result of extended-Hückel molecular-orbital calculations,[17] and subsequently *PRDDO* (partial retention of diatomic differential over-lap) calculations[20] that the $B_8H_8^{2-}$ dodecahedron has nine bonding skeletal molecular orbitals. Figure 4 illustrates how these orbitals are derived from the frontier molecular orbitals of the two D_{2d} distorted B_4H_4 tetrahedra described in some detail above. Eight of the nine orbitals originate from the a_1 and $1t_2$ bonding molecular orbitals of the isolated B_4H_4 tetrahedron. In D_{2d} symmetry these orbitals transform as a_1 and $b_2 + e$ and the union of the two tetrahedra gives rise to the molecular orbitals of $1a_1$, $2a_1$, $1b_2$, $2b_2$, $1e$, and $2e$ symmetry in $B_8H_8^{2-}$. The $2a_1$, $2b_2$, and $2e$ levels represent the out-of-phase combinations of the appropriate molecular orbitals of the B_4H_4 tetrahedra whose antibonding character has been mitigated by interaction with higher-lying orbitals of the same symmetry derived from $1e$, $1t_1$, and $2t_2$. The ninth molecular orbital of the $B_8H_8^{2-}$ ion has b_1 symmetry and is derived primarily from the b_1 component of the $1e$ set in the flattened tetrahedron, and is stabilised by a bonding interaction with the higher-lying b_1 component of the *e* set of the elongated tetrahedron. The lowest-lying antibonding molecular orbital of $B_8H_8^{2-}$ has a_2 symmetry and has a major contribution from the a_2 component of the $1t_1$ molecular orbital of the elongated B_4H_4 tetrahedron.

The requirement for nine skeletal electron pairs in dodecahedral borane clusters is not independent of the substituents attached to the boron atoms. For example, B_8Cl_8 has a structure which is very similar to that of $B_8H_8^{2-}$ although it has one fewer skeletal bonding electron pairs.[4a] An extended-Hückel calculation on B_8Cl_8 has demonstrated that the net effect of the chlorine ligands in this molecule is to raise the energies of the $2a_1$, $1b_1$, $2e$, and $2b_2$ boron skeletal bonding molecular orbitals illustrated in Figure 4 by *ca.* 1.5 eV.* The effect of this change is particularly significant for $2b_2$ since even in $B_8H_8^{2-}$ this lies at substantially higher energies than the $2a_1$, $1b_1$, and $2e$ molecular orbitals. Indeed the corresponding $2b_2$ molecular orbital in B_8Cl_8 lies at higher energies than the boron atomic $2p$ orbital and is consequently not energetically favourable for electron occupation.

Comparison of the Molecular Orbitals for B_4H_4 *and* $M_4(\eta\text{-}C_5H_5)_4$.—In Figure 5 the relative energies of the skeletal molecular orbitals of B_4H_4 and $Co_4(\eta\text{-}C_5H_5)_4$ tetrahedra are compared. The electronic structure of the latter is well understood and has been discussed in

* Throughout this paper: 1 eV $\approx$ 1.60 $\times$ 10^{-19} J.

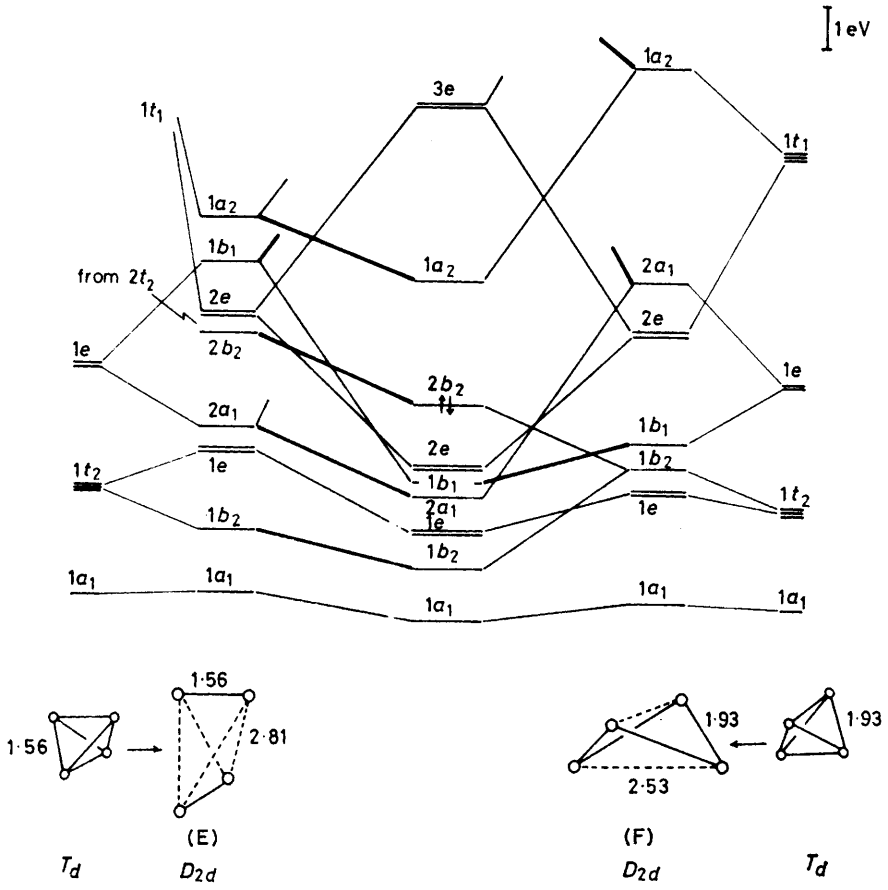

FIGURE 4 Generation of the skeletal molecular orbitals of the $B_8H_8^{2-}$ ion in D_{2d} symmetry by interaction of the molecular orbitals of B_4H_4 tetrahedra which have been elongated or flattened. Bond lengths in Å

some detail in a previous paper [25] in terms of the isolobal nature of $M(\eta\text{-}C_5H_5)$ and B–H. The metal tetrahedron has bonding molecular orbitals of a_1, t_2, and e symmetry and antibonding skeletal molecular orbitals of t_1 and t_2 symmetry in broad agreement with the precepts of the polyhedral skeletal electron-pair approach. However the molecular orbitals of B_4H_4 and $M_4(\eta\text{-}C_5H_5)_4$ differ in the following important respects.

(*i*) The spread of orbital energies for the skeletal molecular orbitals in the metallic cluster is much smaller than that in the borane. This arises in large measure from the smaller interfragment overlap integrals in $M_4(\eta\text{-}C_5H_5)_4$ and reflects the participation of the metal *d* orbitals in this tetrahedron.

(*ii*) The baricentre of the skeletal molecular orbitals lies at lower energies for the metal cluster than the borane tetrahedron reflecting the higher electronegativity of the metal-containing fragments.

(*iii*) The relative energies of the bonding molecular orbitals in the borane and metal tetrahedra follow quite a different ordering. In the former the ordering is $a_1 > t_2 > e$ and in the latter the ordering is $t_2 > e > a_1$. This difference has its origins in the relative energies of the frontier orbitals of the isolated $M(\eta\text{-}C_5H_5)$ and B–H fragments, and in particular the fact that in the former the a_1 orbital lies at significantly higher energies than the *e* orbitals.[25] A similar phenomenon has been noted for the $[Os_3(CO)_{12}]$ cluster and experimentally verified by photoelectron spectral studies.[26]

Having analysed in some detail the effects of distortion on the molecular orbitals of the individual B_4H_4 tetrahedra and made a comparison of borane and metal tetrahedron, we are now in a position to consider the central problem of the bonding interactions in $B_4H_4[M(\eta\text{-}C_5H_5)]_4$ in its two interesting isomeric forms.

$B_4H_4[M(\eta\text{-}C_5H_5)]_4$ *with the Metal Atoms occupying the High-connectivity Sites.*—Since in this isomeric possibility the metalloborane polyhedron is derived from the interaction of an elongated borane tetrahedron and a flattened $M_4(\eta\text{-}C_5H_5)_4$ tetrahedron it is necessary to consider briefly the effect of such a distortion on the metal tetrahedron. As illustrated on the right-hand side of Figure 6 the effect of such a distortion is much the same as that noted previously for the borane polyhedron although the absolute magnitude of the splittings is much smaller. When evaluating the interactions between the metal and borane tetrahedra shown in Figure 6 the fragment electronegativity difference and the smaller spread of energies for the molecular orbitals in

the metal tetrahedra noted above have particularly important consequences.

The metal molecular orbitals derived from $1t_2$, $1e$, a_1, and $1t_1$ of the undistorted tetrahedron are all relatively low lying and have energies comparable to those of the most stable borane molecular orbitals derived of $1a_1$ and $1t_2$ symmetry. Therefore when the molecular orbitals of the metal and borane tetrahedra are allowed to interact the resultant bonding molecular orbitals for B_4H_4-$[M(\eta\text{-}C_5H_5)]_4$ are localised predominantly on the metal atoms and the occupied molecular orbitals reflect in large measure the electronic requirements for stabilising a flattened metal $M_4(\eta\text{-}C_5H_5)_4$ tetrahedron. In particular the closed-shell stable electronic requirement for this isomeric possibility of $B_4H_4[M(\eta\text{-}C_5H_5)]_4$ is eight skeletal electron pairs corresponding to the occupation of the $1a_1$, $1b_2$, $1e$, $1b_1$, $2a_1$, and $2e$ molecular orbitals in Figure 6. These molecular orbitals mirror the symmetries of the molecular orbitals necessary to stabilise an isolated flattened $M_4(\eta\text{-}C_5H_5)_4$ tetrahedron as shown on the right-hand side of Figure 6. The situation is precisely analogous to that described above for P_4Ph_4, where it was noted that the presence of eight skeletal electron pairs would stabilise a flattened tetrahedral structure. In the metalloboranes $B_4H_4[M(\eta\text{-}C_5H_5)]_4$ the B_4H_4 system is effectively acting as an electron sink, by virtue of its lower electronegativity, and providing the necessary electrons to stabilise the flattened $M_4(\eta\text{-}C_5H_5)_4$ structure. The complex $B_4H_4[Co(\eta\text{-}C_5H_5)]_4$ which has eight skeletal electron pairs in total has precisely the right electronic count to fill the eight bonding molecular orbitals $1a_1$, $1b_2$, $1e$, $1b_1$, $2a_1$, and $2e$ in Figure 6. Furthermore, the high-lying nature of the $1a_2$ molecular orbital militates against the formation of a stable $[B_4H_4\{Co(\eta\text{-}C_5H_5)\}_4]^{2-}$ ion.

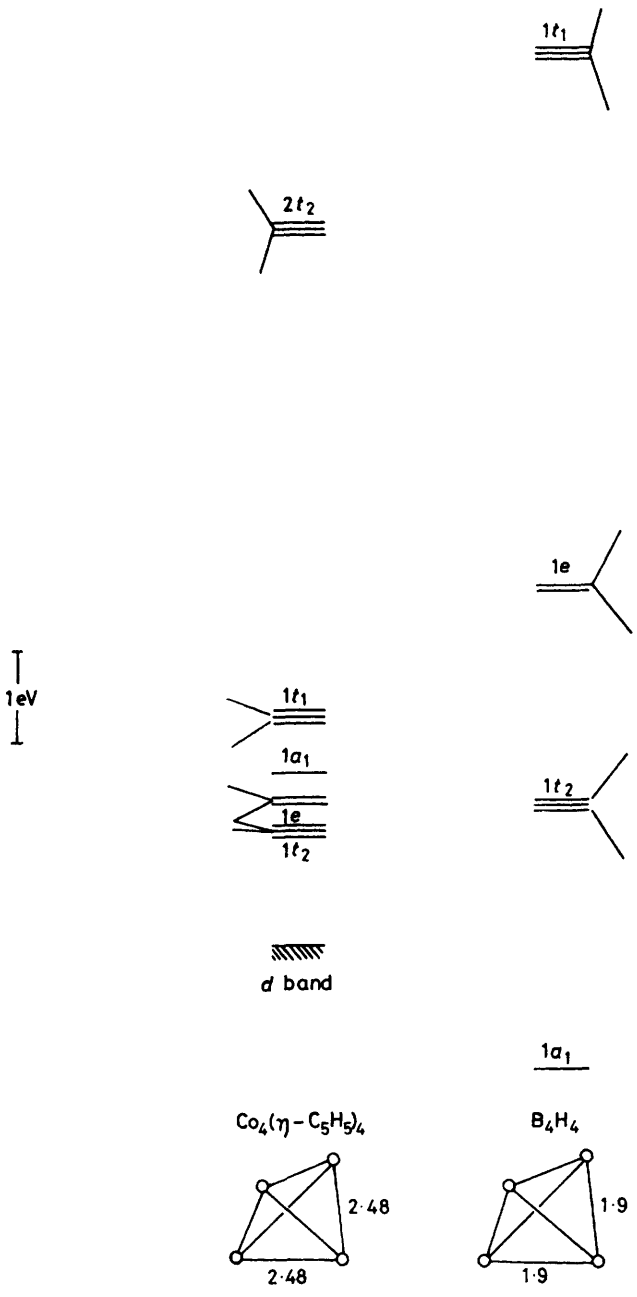

FIGURE 5 Comparison of the relative energies of the skeletal molecular orbitals of $Co_4(\eta\text{-}C_5H_5)_4$ and B_4H_4 tetrahedra. The envelope of orbital energies arising from D_{2d} distortions for each polyhedron is schematically represented. Bond lengths in Å

$B_4H_4[M(\eta\text{-}C_5H_5)]_4$ *with the Metal Atoms occupying the Low-connectivity Sites.*—Figure 7 illustrates the interaction diagram for the union of a B_4H_4 flattened tetrahedron and an elongated $M_4(\eta\text{-}C_5H_5)_4$ tetrahedron to generate the alternative isomeric possibility for B_4H_4-$[M(\eta\text{-}C_5H_5)]_4$. The differences arising from the electronegativity effects and the smaller orbital splittings in the metal tetrahedron are once again apparent in this diagram. The effect of the elongation on the molecular orbitals of the metal tetrahedron bears a strong resemblance to that discussed earlier for the borane tetrahedron. In particular the sense of the splittings observed for the bonding $1t_2$, $1e$, and a_1 molecular orbitals are closely related to those discussed above. In common with the borane, the a_2 and e components of the antibonding $1t_1$ molecular orbital are both stabilised, and the b_2 component of $2t_2$ experiences a very significant stabilisation. The $1a_1$, $2a_1$, $1e$, $1b_2$, $2e$, $2b_2$, $1b_1$, and $1a_2$ bonding molecular orbitals illustrated in Figure 7 for the metalloborane $B_4H_4[M(\eta\text{-}C_5H_5)]_4$ are largely localised on the metal atoms and have their origins in the 10 molecular orbitals of an isolated elongated metal tetrahedron shown on the left-hand side of the Figure. The closed-shell electronic configuration associated with this isomeric possibility corresponds precisely to the electron count found in $B_4H_4[Ni(\eta\text{-}C_5H_5)]_4$, *i.e.* 10 skeletal electron pairs.

An alternative view of this structure is in terms of the B_4H_4 unit acting as a bridging unit between the two Ni_2 components of the Ni_4 elongated tetrahedron. The B_4H_4 bridge contributes four electron pairs to the nickel cluster molecular orbitals which contain six electron

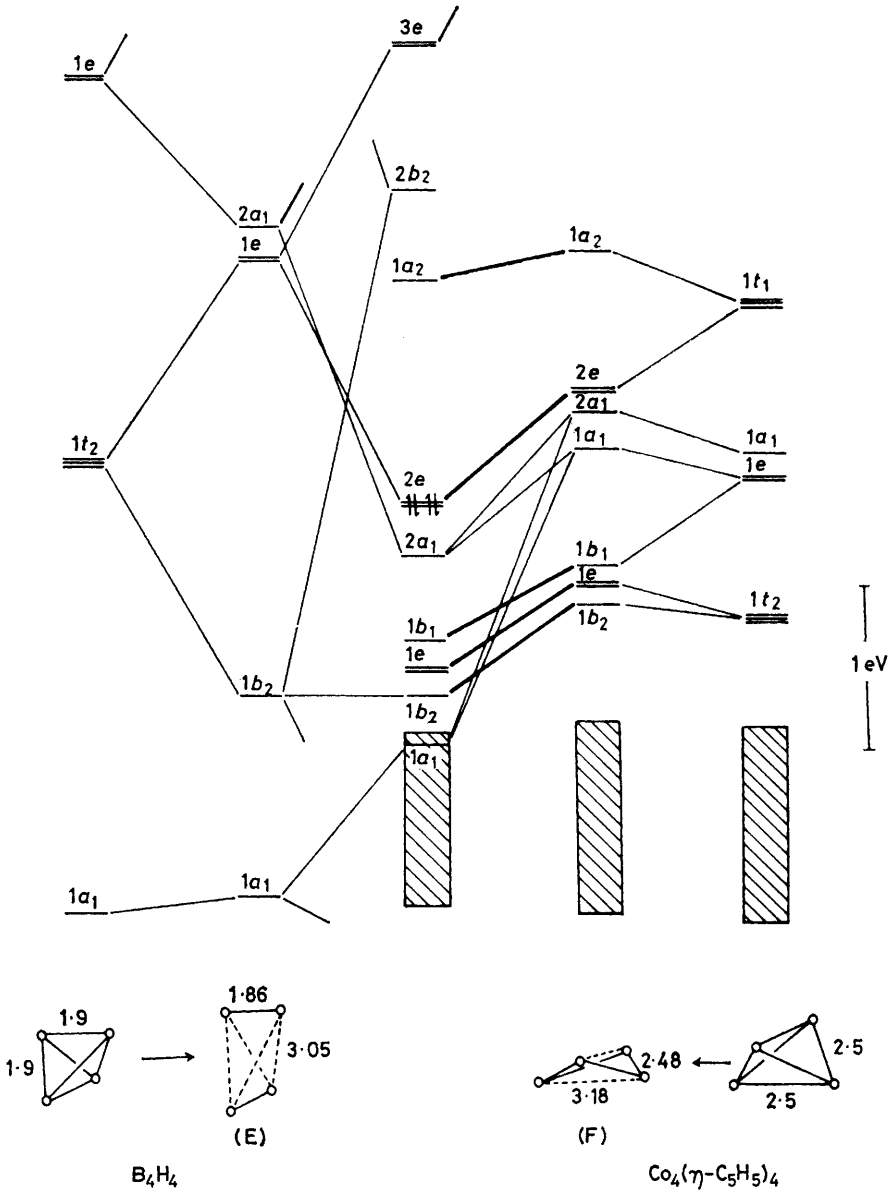

FIGURE 6 Molecular-orbital interaction diagram for an elongated B_4H_4 tetrahedron (E) and a flattened $Co_4(\eta\text{-}C_5H_5)_4$ tetrahedron (F) to generate the molecular orbitals of $B_4H_4[Co_4(\eta\text{-}C_5H_5)_4]$. The hatched areas represent the metal *d* band of molecular orbitals. The highest-occupied molecular orbitals are indicated by the antiparallel pairs of arrows. Bond lengths in Å

pairs donated by the $Ni(\eta\text{-}C_5H_5)$ fragments. The additional electron pairs stabilise the elongated tetrahedral structure, since as we have noted previously 10 electron pairs are required to effectively stabilise the elongated tetrahedron. According to this view $B_4H_4[Ni(\eta\text{-}C_5H_5)]_4$ bears a formal relationship to $[Fe_4(\eta\text{-}C_5H_5)_4S_4]$, which also has 10 skeletal electron pairs. The iron atoms in this cluster also adopt an elongated D_{2d} tetrahedral geometry.[27]

The qualitative arguments developed above have been fully substantiated by extended-Hückel molecular-orbital calculations on the model compounds $[B_4H_4(CoL_3)_4]^{4+}$ and $B_4H_4(CoL_3)_4$, where L is a two-electron σ-donating ligand. Complete details concerning the parameters and geometries used in these calculations are described in the Appendix. These compounds are isoelectronic with $B_4H_4[Co(\eta\text{-}C_5H_5)]_4$ and $B_4H_4[Ni(\eta\text{-}C_5H_5)]_4$ respectively. For the cobalt complex the isomer with the metal atoms occupying the high-connectivity sites is preferred by 2.2 eV, whereas in the nickel complex the isomer with the metal atoms occupying the low-connectivity sites is preferred by 3.4 eV. Clearly, even taking into account the crudity of this type of calculation and the need to approximate the $M(\eta\text{-}C_5H_5)$ units by ML_3 fragments, these represent rather large energy differences and its seems most likely that the observed structures for $B_4H_4[Co(\eta\text{-}C_5H_5)]_4$ and $B_4H_4[Ni(\eta\text{-}C_5H_5)]_4$ represent the thermodynamically preferred structures.

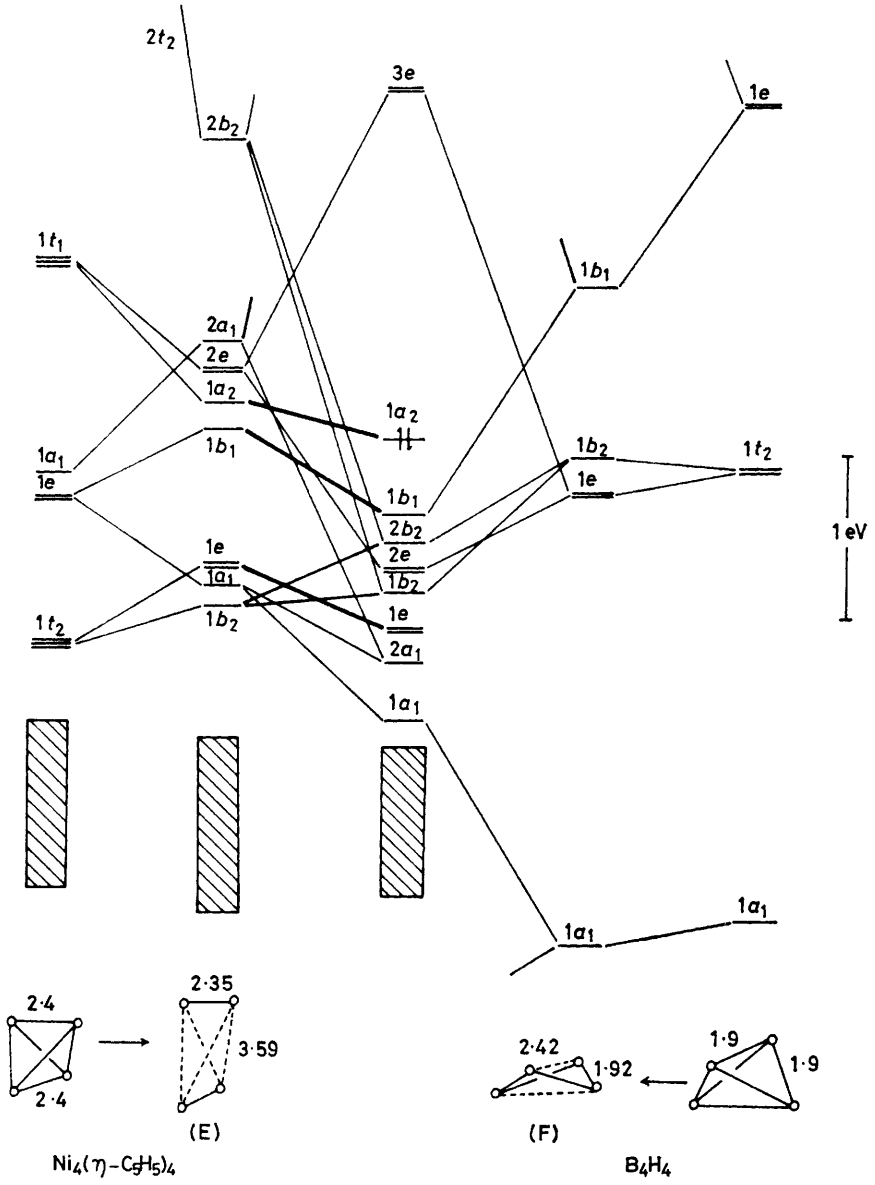

FIGURE 7 Molecular-orbital interaction diagram for an elongated $Ni_4(\eta\text{-}C_5H_5)_4$ tetrahedron (E) and a flattened B_4H_4 tetrahedron (F) to generate the molecular orbitals of the $B_4H_4[Ni(\eta\text{-}C_5H_5)]_4$ dodecahedron. The highest-occupied molecular orbital is indicated by the pair of antiparallel arrows. Bond lengths in Å

Orbital-correlation diagrams for the interconversion of the isomeric possibilities of $B_4H_4[Co(\eta\text{-}C_5H_5)]_4$ and $B_4H_4[Ni(\eta\text{-}C_5H_5)]_4$ through D_{2d} square-antiprismatic structures have established that the processes are symmetry allowed.[28] Therefore, if the two isomeric possibilities for either $B_4H_4[Co(\eta\text{-}C_5H_5)]_4$ or $B_4H_4[Ni(\eta\text{-}C_5H_5)]_4$ had similar energies then one would anticipate that their interconversion would have a low activation energy. However, the large computed energy differences (*i.e.* 2.2 and 3.4 eV for the cobalt and nickel complexes respectively) for the isomers make such interconversions thermodynamically unfavourable.

An alternative view of the site preferences exhibited by the metal atoms in the dodecahedral molecules may be gained by considering the charge distribution in the following series of molecules and ions based on the parent dodecahedral B_8H_8 unit. Since the highest-occupied and lowest-unoccupied molecular orbitals in the $B_8H_8^{2-}$ ion are both predominantly localised on the low-connectivity site boron atoms there is an overall build up

	B_8H_8	$B_8H_8^{2-}$	$B_8H_8^{4-}$
No. of skeletal electron pairs	8	9	10
Atomic charges			
Low-connectivity boron atoms	+0.3	−0.1	−0.5
High-connectivity boron atoms	+0.2	+0.1	0.0

of negative charge on these boron atoms as one proceeds from B_8H_8 to $B_8H_8^{2-}$ to $B_8H_8^{4-}$. If it is recognised that the $M(\eta\text{-}C_5H_5)$ fragment has a higher effective electronegativity than the B–H fragment, see (*ii*) on p. 1792, then it follows from first-order perturbation-theory arguments that the metal atoms will occupy those sites of the polyhedron which have the more negative atomic charges. For dodecahedral molecules derived from B_8H_8 with eight skeletal electron pairs, *e.g.* $B_4H_4[Co(\eta\text{-}C_5H_5)]_4$, the high-connectivity sites are preferred by the metal atoms since these sites bear a less positive atomic charge. Similarly, for dodecahedral species derived from $B_8H_8^{4-}$ with 10 skeletal electron pairs, *e.g.* $B_4H_4[Ni(\eta\text{-}C_5H_5)]_4$, then it is the low-connectivity sites which are preferred for metal occupation. Therefore, such an electronegativity argument can clearly account for the observed isomers of the metalloboranes, although it does not provide any appreciation of why the nickel and cobalt complexes both form *closo*-dodecahedral clusters.

In common with $B_4H_4[Ni(\eta\text{-}C_5H_5)]_4$, a hypothetical $C_4B_4H_8$ dodecahedron would also possess 10 skeletal electron pairs and a similar electronegativity argument leads to the prediction that the more stable isomer has the carbon atoms in the low-connectivity sites. Fehlner,[29] however, has proposed from n.m.r. studies that a C_4B_4 skeletal system adopts a more open *nido*-structure rather than one based on a dodecahedron.

A comparison of the frontier molecular orbitals of $B_8H_8^{2-}$ and symmetry-equivalent orbitals of $B_4H_4[Ni(\eta\text{-}C_5H_5)]_4$ and a dodecahedral $C_4B_4H_8$ is shown in Figure 8. This suggests that the difference between

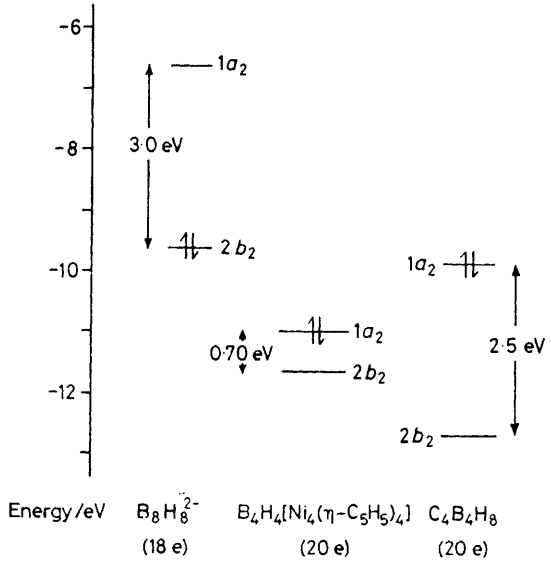

FIGURE 8 Comparison of the energies of the frontier molecular orbitals of $B_8H_8^{2-}$, $B_4H_4[Ni(\eta\text{-}C_5H_5)]_4$, and $C_4B_4H_8$

$B_4H_4[Ni(\eta\text{-}C_5H_5)]_4$ and $C_4B_4H_8$ has its origins in the $1a_2$ molecular orbital, which is localised predominantly on the low-connectivity atoms, Ni and C respectively.

The $1a_2$ orbital is antibonding between the atoms at these sites but the large C–C $2p$ overlap integrals in $C_4B_4H_8$ compared to the corresponding Ni–Ni overlaps in $B_4H_4[Ni(\eta\text{-}C_5H_5)]_4$ result in a greater antibonding character for this orbital in the carborane. This antibonding character is reflected in the lower computed C–C overlap population of 0.6 in $C_4B_4H_8$ compared to that of 0.8 for comparable boron atoms in $B_8H_8^{2-}$. It results in a destabilisation of the dodecahedral structure relative to alternative *nido*-structures for $C_4B_4H_8$. We are currently investigating the relative stabilities of the alternative *nido*- and *arachno*-structures for $C_4B_4H_8$ and will discuss them in a forthcoming publication.

APPENDIX

All the calculations were performed using the extended-Hückel method,[23,30] and the relevant orbital parameters are summarised in the Table. These parameters have been

Parameters for molecular-orbital calculations

Atomic orbital	H_{ii}/eV	Slater exponent	Ref.
Co 4*s*	−10.21	2.0	*a*,*b*
Co 4*p*	−7.29	2.0	*a*,*b*
B 2*s*	−15.2	1.3	*c*
B 2*p*	−8.5	1.3	*c*
H 1*s*	−13.6	1.3	*c*
Cl 3*s*	−30.0	2.033	*c*
Cl 3*p*	−15.0	2.033	*c*
C 2*s*	−21.4	1.625	*c*
C 2*p*	−11.4	1.625	*c*

	H_{ii}/eV	ξ_1	C_1	ξ_2	C_2	Ref.
Co 3*d* function	−13.18	5.55	0.5680	2.10	0.6060	*a*,*b*

[a] J. W. Richardson, W. C. Nieuwport, R. R. Powell, and W. F. Edgell, *J. Chem. Phys.*, 1962, **36**, 1057. [b] H. Basch and H. B. Gray, *Theor. Chim. Acta*, 1966, **4**, 367. [c] R. Hoffmann, *J. Chem. Phys.*, 1963, **39**, 1397.

found to be satisfactory in predicting molecular geometries of organometallic compounds.[5] The off-diagonal terms H_{ij} were estimated in the usual fashion from $H_{ij} = kS_{ij}(H_{ii} + H_{jj})/2$ with $k = 1.75$.[23] Computer size limitations prevented calculations on the molecules $B_4H_4[M(\eta\text{-}C_5H_5)]_4$ and therefore the $M(\eta\text{-}C_5H_5)$ fragment was modelled by an ML_3 fragment, where L is a two-electron ligand with orbital exponent equal to that of the hydrogen 1*s* orbital and an H_{ii} of −12.6 eV. This fragment, when used in conjunction with the metal parameters given in the Table, was found to simulate the frontier molecular orbitals of an $M(\eta\text{-}C_5H_5)$ fragment and the tetrahedral cluster $M_4(\eta\text{-}C_5H_5)_4$ very closely, both in terms of energy and orbital composition.[25]

The skeletal geometries for the calculations on $B_8H_8^{2-}$, B_8Cl_8, $C_4B_4H_8$, $[B_4H_4(CoL_3)_4]^{4+}$, and $B_4H_4(CoL_3)_4$ were derived from published *X*-ray crystallographic data on $B_8H_8[Zn(NH_3)_4]$, $B_4H_4[Co(\eta\text{-}C_5H_5)]_4$, and $B_4H_4[Ni(\eta\text{-}C_5H_5)]_4$ as illustrated in Figure 1.[17,20,21]

Non-bonded cage distances and terminal-atom bond lengths are (*a*) for $B_8H_8^{2-}$, B_8Cl_8, and $C_4B_4H_8$: (*i*) between low-connectivity sites 2.81 Å; (*ii*) between high-connectivity sites 2.53 Å; B–H 1.19; C–H 1.19; B–Cl 1.72 Å. (*b*) For the metalloboranes: (*i*) in $B_4H_4[Co(\eta\text{-}C_5H_5)]_4$ B · · · B 3.05 and Co · · · Co 3.18 Å; (*ii*) in $B_4H_4[Ni(\eta\text{-}C_5H_5)]_4$

Ni · · · Ni 3.59 and B · · · B 2.42 Å; B–H 1.19; M–L 1.6; L–M–L 90°. The calculations were made on the ICL 2980 computer at Oxford University using the programs ICON 8 and FMO.[30]

We thank the S.R.C. for a studentship (to D. N. C.) and the Scientific Affairs Division of N.A.T.O. for providing funds to enable D. N. C. to study at Cornell University for 2 months.

[0/1420 *Received*, 15*th September*, 1980]

REFERENCES

[1] M. F. Hawthorne, *J. Organomet. Chem.*, 1975, **100**, 97.
[2] R. N. Grimes, *Acc. Chem. Res.*, 1978, **11**, 420.
[3] F. G. A. Stone, *J. Organomet. Chem.*, 1975, **100**, 257.
[4] (*a*) K. Wade, *Adv. Inorg. Chem. Radiochem.*, 1976, **18**, 1; (*b*) D. M. P. Mingos, *Nature Phys. Sci.*, 1972, **236**, 99; (*c*) R. W. Rudolph, *Acc. Chem. Res.*, 1976, **9**, 446; (*d*) R. N. Grimes, *Ann. N. Y. Acad. Sci.*, 1974, **239**, 180.
[5] D. M. P. Mingos, *Adv. Organomet. Chem.*, 1977, **15**, 1.
[6] M. Elian and R. Hoffmann, *Inorg. Chem.*, 1975, **14**, 1058; M. Elian, M. M. L. Chen, D. M. P. Mingos, and R. Hoffmann, *ibid.*, 1976, **15**, 1148.
[7] D. M. P. Mingos, *J. Chem. Soc., Dalton Trans.*, 1977, 602.
[8] D. M. P. Mingos, *J. Chem. Soc., Dalton Trans.*, 1977, 610.
[9] J. Evans, *J. Chem. Soc., Dalton Trans.*, 1978, 18.
[10] D. M. P. Mingos, *Pure Appl. Chem.*, 1980, **52**, 705.
[11] R. Hoffmann, T. A. Albright, and D. L. Thorn, *Pure Appl. Chem.*, 1978, **50**, 1.
[12] D. M. P. Mingos, M. I. Forsyth, and A. J. Welch, *J. Chem. Soc., Chem. Commun.*, 1977, 605.
[13] D. M. P. Mingos and M. I. Forsyth, *J. Organomet. Chem.*, 1978, **148**, C37; D. M. P. Mingos, M. I. Forsyth, and A. J. Welch, *J. Chem. Soc., Dalton Trans.*, 1978, 1363.
[14] D. M. P. Mingos and A. J. Welch, *J. Chem. Soc., Dalton Trans.*, 1980, 1674.
[15] T. A. Albright and R. Hoffmann, *Chem. Ber.*, 1978, **111**, 1578.
[16] J. W. Lauher, M. Elian, R. H. Summerville, and R. Hoffmann, *J. Am. Chem. Soc.*, 1976, **98**, 3219.
[17] L. J. Guggenburger, *Inorg. Chem.*, 1969, **8**, 2771; F. Klanberg, D. R. Eaton, L. J. Guggenberger, and E. L. Muetterties, *ibid.*, 1967, **6**, 1271.
[18] E. L. Muetterties, R. J. Wiersema, and M. F. Hawthorne, *J. Am. Chem. Soc.*, 1973, **95**, 7520.
[19] E. I. Tolpin and W. N. Lipscomb, *J. Am. Chem. Soc.*, 1973, **95**, 2384.
[20] D. A. Kleir and W. N. Lipscomb, *Inorg. Chem.*, 1979, **18**, 1312.
[21] J. R. Pipal and R. N. Grimes, *Inorg. Chem.*, 1979, **18**, 257.
[22] J. R. Bowser, A. Bonny, J. R. Pipal, and R. N. Grimes, *J. Am. Chem. Soc.*, 1979, **101**, 6229.
[23] R. Hoffmann and W. N. Lipscomb, *J. Chem. Phys.*, 1962, **36**, 2179.
[24] D. S. Urch and A. G. Massey, *J. Chem. Soc.*, 1965, 6180.
[25] R. Hoffmann, B. E. R. Schilling, R. Bau, H. D. Kaesz, and D. M. P. Mingos, *J. Am. Chem. Soc.*, 1978, **100**, 6088.
[26] J. C. Green, E. A. Seddon, and D. M. P. Mingos, *J. Chem. Soc., Chem. Commun.*, 1979, 94.
[27] C. H. Wei, G. R. Wilkes, D. M. Treichel, and L. F. Dahl, *Inorg. Chem.*, 1966, **5**, 900.
[28] R. B. Woodward and R. Hoffmann, ' Conservation of Orbital Symmetry,' Academic Press, New York, 1969.
[29] T. P. Fehlner, *J. Am. Chem. Soc.*, 1980, **102**, 3424.
[30] J. Howell, A. Rossi, D. Wallace, K. Haraki, and R. Hoffmann, Quantum Chemistry Program Exchange, 1977, **10**, 344.